The influence of unsaturated phenomena in the failure of an ancient (upstream raised) tailings dam

Luciano A. Oldecop[1], Rubén D. Rodari[1], Lucas Garino[1], Gustavo Navarta[1]

[1]*Instituto de Investigaciones Antisísmicas "Ing. Aldo Bruschi", Facultad de Ingeniería, Universidad Nacional de San Juan, Argentina.*

**Corresponding author's email: oldecop*@unsj.edu.ar

Abstract: A back analysis of a failure case of a small ancient tailings dam that occurred some 60 years ago was attempted with limited success. Upper Castaño Viejo is the only flow failure of a tailings deposit that occurred in Argentina. The data for the analysis were collected from oral accounts, field exploration campaigns, and laboratory testing. A finite element seepage model and limit equilibrium analysis were used for trying to reproduce the failure process. Ancient tailings dams like the study case can be assimilated to the upstream-raised typology. A vast number of such facilities, remains of past mining activities, exist in a variety of care conditions. Hence, a better understanding of their failure mechanisms is certainly relevant. In the case presented, the malfunctioning of a decant pipe was primarily suspected to have caused the failure. However, reproducing the failure process was not straightforward. Additional hypotheses had to be introduced. Among the several factors analysed, the retention curve, unsaturated permeability, anisotropy, and surficial desiccation were found to possibly play a significant role in the failure process. It is concluded that upstream raised dams are extremely complex systems, a fact that could explain our limited ability to forecast their performance.

Introduction

Many ancient tailings dams like the study case presented in this paper (i.e., those built before the 1970's) can be assimilated to the upstream-raised typology. The only difference is that no borrow material was used in the heightening lifts, but the tailings coarse fraction [1,2]. There is an ongoing debate about the inherent dangers of upstream raised tailings dams and a growing consensus that this typology should be phased out, especially in seismically active countries [3, 4]. Nevertheless, several mines all over the world use upstream raised dams. Moreover, the upstream-raised typology is likely to be considered for new projects because it is still the least expensive technology for tailings disposal [6]. Aside from the debate, a vast number of such facilities, remains of past mining activities, exist in a variety of care conditions [7, 8]. Many of them remain in total abandonment [9, 10]. Hence, a better understanding of their behaviour and their failure mechanisms is certainly relevant at present, regarding public safety and environmental care. While performing the analysis of failure cases it becomes clear that static liquefaction plays a primary role in generating the catastrophic consequences frequently observed, i.e. high-speed mud avalanches travelling

many kilometres downstream. On the other hand, it is usually much less evident what was the triggering mechanism of each failure case, i.e. the set of factors and processes leading the structure to attain the unstable condition required for liquefaction to initiate [11-13].

The goal of this work is to improve the knowledge about the behaviour and safety of upstream raised tailings dams.

The study case: Upper Castaño Viejo Dam

Mining operations and dam geometry

The Castaño Viejo Dam is located in the Andes range at 2300 m.a.s.l., San Juan Province, Argentina (Lat 30º57' S, Long 69º38' W). The site is quite remote, currently no accessible with four-wheeled vehicles. The mining operations lasted from 1955 to 1964. Lead, zinc, copper and silver were extracted with a flotation process. The ore was obtained from an underground work and treated in a plant located nearby the mine. The mine was notably important for the time; worth it was the building of a small town housing some 500 workers. Due to space limitations, the tailings were hydraulically deposited in twenty-three small dams distributed over 10 km downstream along a narrow gorge. A small creek, with some permanent springs and occasional runoff of rainfall water, runs through the valley bottom.

The dam selected as study case is the one located most upstream among the multiple tailings deposits, located just next to the extraction plant. The dam sits directly in the streambed, which is notably steep, nearly 7%. Figure 1 displays a panoramic picture of the dam site in its current condition. The relicts left after the accident can still be observed and interpreted with reasonable accuracy, in spite of the 50+ years of natural degradation, thanks to the arid climate. A topographical survey and a geotechnical exploration campaign were carried out. This allowed rebuilding the dam's original geometry at the time of the accident with most of its details (Figure 2).

Figure 1: Photo of the Upper Castaño Viejo Dam site. Extreme left: starter dam location. Center: sliding surface. Extreme right: decant pond location.

The starter dam was placed taking advantage of a natural narrows, owing to the presence of an igneous dyke (extreme left of the photo in Figure 1). The dam main slope was raised by

using the same tailings. The raising method involved sinking wooden logs in the previously placed tailings, which supported horizontal planks acting as scaffold for the next lift [2]. Once the coarse tailings attained some degree of mechanical strength by air-drying the scaffolding planks were removed and reused. The resulting deposit has no actual "dam body", but a zone of coarse tailings next to the main slope, which harnesses the strength due desiccation for achieving the stability of the deposit. The impoundment has a 0.6 ha footprint and an estimated volume of 24000 m^3. The height of the main slope (before failure) was 11.3 meters between the toe of the starter dam and the tailings crest. The main slope was notably steep (36º). Despite being swept almost all by the failure slide, the slope position and inclination could be precisely measured from the tailings relics still adhered to both abutments.

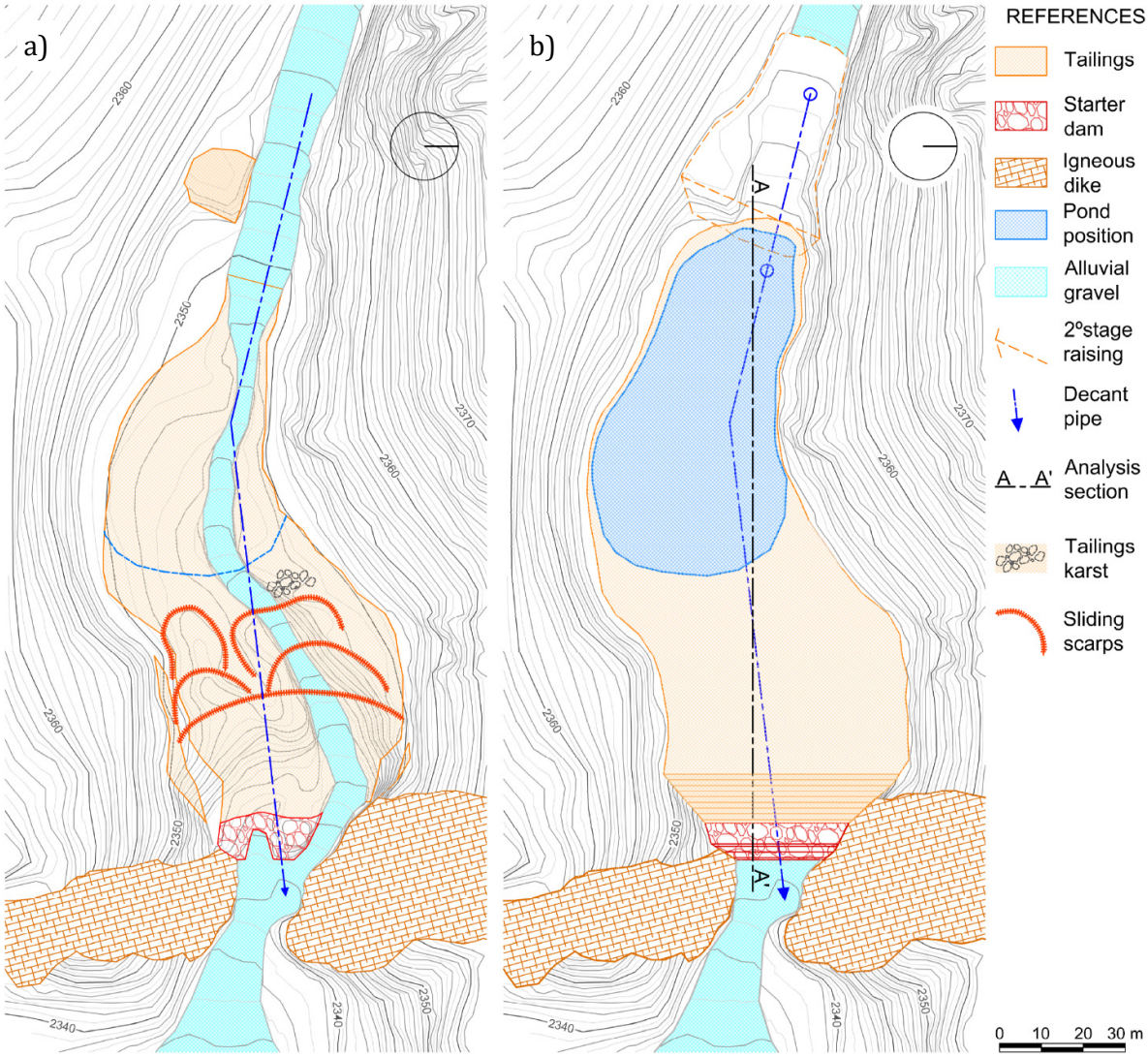

Figure 2: Plan view of Upper Castaño Viejo Dam. a) Current state of the relicts. b) Geometry of the dam before the accident restored from the field surveys.

The 2.7-meter-high starter dam was built with rock blocks ranging from 3" to 20" in diameter. Within a zone located upstream, the rockfill voids appear totally clogged by the

tailings (Figure 3a). The mechanism which led to this is not clear. Either the fluid tailings of the first pours seeped through the rockfill large voids, owing to the lack of filter, or rockfill and tailings were co-disposed on purpose.

The decant system consisted of a precast concrete pipe 200 mm in diameter directly laid over the alluvial material at the valley bottom. Some sections of such pipe remain visible (Figure 3b). The system was completed with vertical steel pipes acting as decant towers, connected with the horizontal conduit. One of those pipes (75 mm in diameter) was found protruding from the ground at the farthest upstream limit of the deposit.

The remains of a smaller second deposit (only 2 meters high above the stream bed) where found immediately upstream of the decant pond (Figure 2). The relicts are almost completely erased by the erosion. It is likely that the two deposits shared the same decant system. Moreover, the presence of this second deposit or raise, is an indication that the main deposit was probably no longer operative but as common in these cases, still holding water on top of the tailings in the pond zone.

Figure 3: a) Starter dam. Note the rockfill voids invaded by tailings. b) 200 mm precast concrete pipe laid in the valley bottom as decant pipe.

The climate at the site is rather arid. The mean annual temperature and relative humidity are 13.6ºC and 31%, respectively. The mean annual precipitation is 150 mm while the annual potential evapotranspiration was estimated in 1250 mm [14]. The hydric deficit prevails, all year round. Most of the rainfall occurs during summer from convective storms, having high intensity and short duration. Snow precipitations are minor, only 20 mm of water equivalent in the year, and snow accumulation rarely persists for more than a couple of days.

The accident

The case studied is the only flow failure of a tailings dam in Argentina's mining history. The case remained mostly unnoticed, probably because of the small volume of both the dam and the spill and because of the remoteness of its location. There are no written records of the accident but only oral accounts, and its exact date is unknown. The failure was followed by

an avalanche of liquified tailings that moved at least 3 km downstream, according to both the field observations and the oral reports. Several tailings slackwater deposits (Figure 4a), still discernible along the river's course, indicate that at some sections the mud flood reached at least 2m above the streambed. The steep slope of the valley also suggests that the escaped tailings mass has travelled downstream at high speed. Tales are that a truck travelling on the mine access road was engulfed by the avalanche. Some versions suggest that three people riding the vehicle died, while others say they narrowly escaped by climbing the riverside slope. An estimation of the tailings volume escaped in the accident, based on the topographical data gathered in the field, yielded an approximate figure of 11000 m^3.

Two mechanisms are the most likely triggers of the dam failure: 1) overtopping during a flood or, 2) slope instability triggered by a malfunction of the decant system. Regarding the first mechanism, flash floods are likely to occur upon summer convective storms. Moreover, to our knowledge, the facility had no spillway or other discharge structure than the decant pipe. However, some details make the overtopping hypothesis less likely. For instance, in a case of overtopping, a breach localized in a limited width of the dam would be expected rather than the observed circular sliding surface spanning all the dam width (Figure 4b).

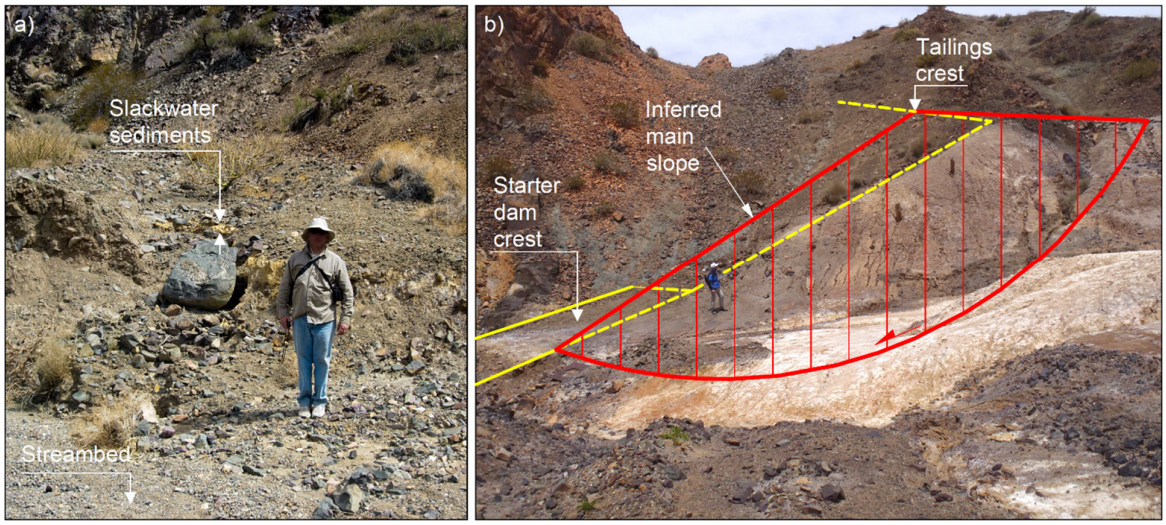

Figure 4: a) Slackwater deposits from the tailings avalanche located some 750m downstream the dam site. b) Main slope zone, with indication of the inferred initial sliding surface.

Otherwise, there is compelling evidence supporting the second hypothesis. The type of connections between the sections of the precast concrete decant pipe are rather weak and prone to leak. This type of conduit is designed to work as an open channel. Given its observed location, it is highly probable that a large section of the pipe was permanently embedded in saturated tailings. Leaks from the tailings into the pipe could lead to the migration of solid particles and hence the possibility of developing piping and the eventual formation of caverns and sinkholes. These are indeed the type of features found at the location indicated in the plan shown in Figure 2.a. A network of caverns and sinkholes (Figure 5) was found a couple of meters away from the decant pipe trace and about 60 m upstream of the starter dam axis. The karstic features cover an area of no more than 50 sqm. It is worth noting that

there is no other place within the deposit with such characteristics, which reinforces the hypothesis that the observed piping signs were related to leaks into the decant conduit and not by other causes (dissolution, for instance). Although failure seems neither to have been caused by the piping process itself.

The escaping solid particles from the decant pipe could have led to pipe clogging downstream of the leaking point. A partial obstruction would have increased the water depth within that pipe section, causing a decrease in flow velocity. This, in turn, would have enhanced particle sedimentation, continuing the clogging process until the upstream pipe cross-section was put under pressure. At this point, the leak was reversed, and the pipe started injecting water into the tailings. The pressure within the pipe could have risen to the pressure head determined by the pond level. This meant a shortcut of the hydraulic head dissipation path, which eventually destabilized the deposit. Importantly, an observer would have had no notice of these ongoing events, as the flow at the downstream end of the pipe would have always appeared normal.

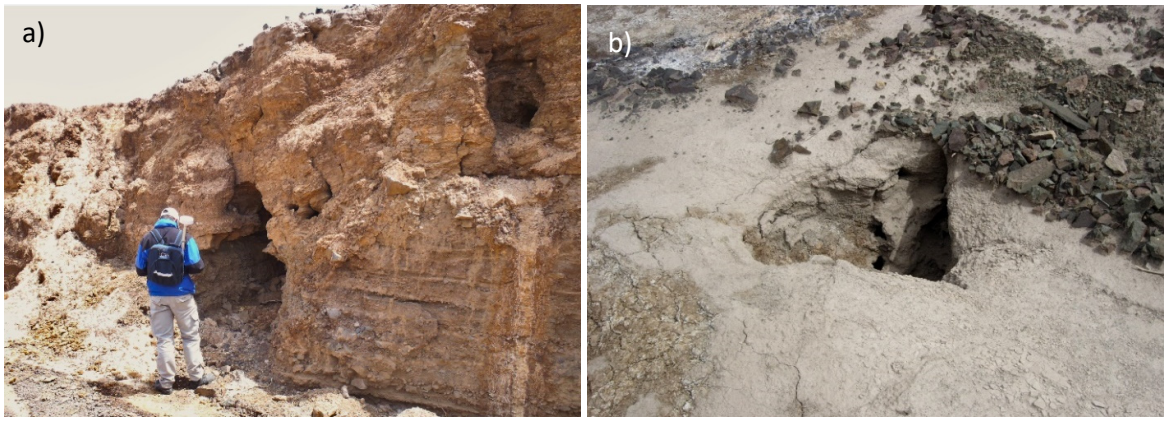

Figure 5: a) Caverns presumably formed by piping due to leaks into the decant pipe. Note bending of the strata above the cavern roof. b) Sinkhole found at the top of the tailings beach in correspondence with the caverns shown in Figure 5a.

Materials

Given the difficulties for accessing the site, it was impossible to conduct a complete exploration program in the studied dam. Instead, a reduced number of representative samples were collected and compared with samples from other tailings deposits also pertaining to the mine. This allowed verifying that all deposits contain similar tailings. Two of them, located 5 Km downstream, were accessible by off-road vehicle. Therefore, exploration campaigns were performed there, which included surface sampling, bore logging and sampling, standard penetration tests (SPT), in-situ permeability tests, shear wave velocity and electrical resistivity tomography [9, 14, 15]. The data collected in those campaigns are used here under the assumption that they are representative of the case studied.

Physical Properties

The grain size distribution (GSD) varies within the deposit because of the hydraulic filling method used. The material becomes finer as the sampling point moves away from the discharge points, which in this case were located along the dam crest. Strong vertical variations in grain size are also common, owing to the stratified structure of the deposit. A simplified distribution of materials is adopted for modelling purposes. Three distinct types of tailings are considered, each type pertaining to a zone within the deposit: (1) the discharge zone, (2) the beach zone, and (3) the decant pond zone. The index properties are summarized in Table 1. Figure 6 shows the average grain size distribution for each zone.

Table 1: Physical and index properties of Castaño Viejo tailings [14].

DEPOSIT ZONE	*Discharge*	*Beach*	*Pond*
Distance ranges from discharge point [m]	*0-5*	*5-55*	*55-127*
Classification (USCS)	*SM*	*SM/ML*	*ML/CL*
Specific gravity, G_s	*2.91*	*2.83*	*2.68*
Dry unit weight, γ_d [kN/m^3]	*14.8*	*15.0*	*13.7*
Porosity/Void ratio, e	*0.48/0.93*	*0.46/0.85*	*0.44/0.79*
LL / PL [%]	---	---	*35/21*
Finer than #200 [%]	*37*	*66*	*95*
D_{60} [mm]	*0.114*	*0.056*	*0.023*
D_{50} [mm]	*0.094*	*0.040*	*0.019*
D_{30} [mm]	*0.061*	*0.024*	*0.014*
D_{10} [mm]	*0.029*	*0.015*	*0.012*
Cu	*4.58*	*3.75*	*1.84*

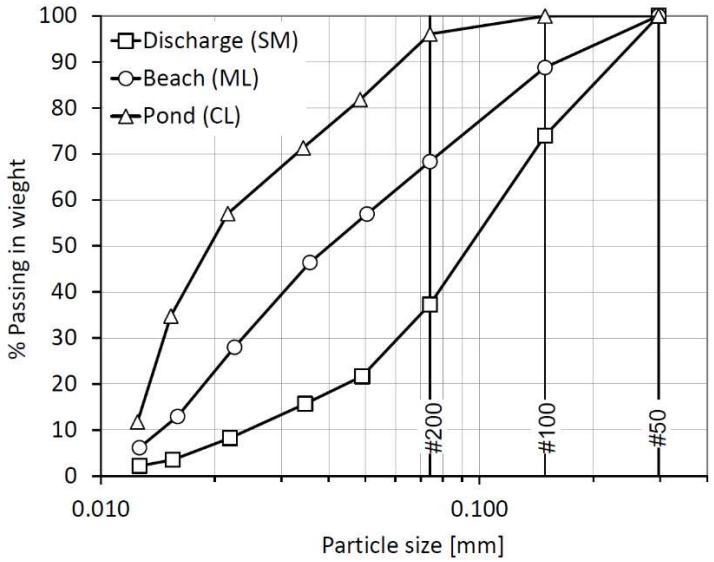

Figure 6: Mean grain size distribution curves from samples collected in the three zones of the deposit: discharge zone, beach zone and decant pond zone.

Permeability

Tailings have a marked stratified structure (Figure 7). This makes their hydraulic properties particularly challenging to characterize. The saturated permeability was measured with in-situ measurements using a Boutwell permeameter (ASTM D6391-11, Method B) [16] at the points indicated in Table 2, along with their distance from the discharge point (dam crest). Moreover, bulk samples were also collected at the same points and laboratory permeability tests were conducted on remoulded specimens using a flexible wall permeameter [17]. Laboratory specimens were prepared by wet tamping at the mean dry unit weight measured in the field (indicated in Table 1).

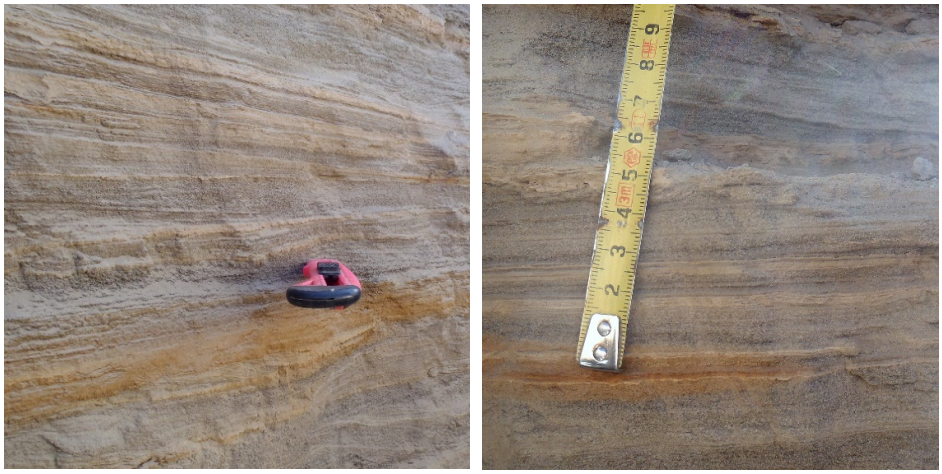

Figure 7: Stratification of Castaño Viejo tailings. Photos taken in exploration pits. Millimetric stratification alternates fine sand and silt layers. Some layers exhibit oxidation.

As indicated in Table 2, the laboratory permeability measurements yielded values between 6 and 30 times lower than the field measurements. A possible explanation for this apparent discrepancy could be that field measurements are performed on the porous media with its stratified structure unaltered. Otherwise, in laboratory measurements, the sampling process makes all the grain size fractions from different strata be mixed up. Therefore, it is reasonable to expect that measurements on reconstituted specimens yield lower values, since permeability is mostly controlled by the finer fraction of the sampled material.

Two additional laboratory tests were conducted with the goal of investigating the effect of desiccation on the hydraulic conductivity of the tailings from the discharge zone and from the beach zone. Specimens were prepared in cylindrical moulds starting from a slurry consistency and left exposed to air-drying until the water content was constant. The mean temperature and RH in the laboratory environment are 22ºC and 35%, respectively. The resulting initial water content was 3% for the discharge zone sand and 8% for the silt from the beach. The permeability measurements show a reduction of one order of magnitude for the air-dried specimens in comparison with those tested in normal initial conditions. The effect can be attributed to two possible effects of desiccation: pore volume decrease by shrinkage and salt precipitation within the material pores. During the exploration

campaigns, ample evidence of salt precipitation was certainly observed (see Figure 1, for instance).

Table 2. Permeability measurements of Castaño Viejo tailings in [m/s]. In-situ measurements after Garino 2018 [14].

DEPOSIT ZONE	*Discharge*	*Beach*	*Pond*
Distance from discharge point [m]	*2*	*26*	*65*
Boutwell Permeameter (ASTM6391-11, Method B)	*9.75E-07*	*1.71E-07*	*6.17E-08*
Flexible wall permeameter (wet tamped specimen)	*1.51E-07*	*5.78E-09*	*2.49E-09*
Flexible wall permeameter (air-dry specimen)	*1.40E-08*	*6.23E-10*	---

Tailings Retention Curve

Retention curves were determined for samples taken from the discharge zone and the beach zone. The retention curve for the pond zone material is not relevant in this case, as this material remains saturated throughout the entire analysis. Two complementary techniques were used: the filter paper method [18] and measurements with a UMS-T5X tensiometer [14]. The results are presented in Figure 8, showing matric suction versus degree of saturation ($S = \theta/\theta_s$, where θ is volumetric water content, and θ_s is the saturation volumetric water content or porosity). For each laboratory dataset, van Genuchten curves were fitted [19]:

$$\theta = \theta_r + (\theta_s - \theta_r)/\left\{1 + \left[\alpha\left(p_g - p_l\right)\right]^n\right\}^m \quad (1)$$

where θ_r is the residual volumetric water content, p_g and p_l are the gas phase and liquid phase pressures, respectively, and α, n, and m are fitting parameters whose values are given in Table 3. In addition to laboratory data, Figure 8 includes a series of points obtained from field measurements [15]. These data (over 30,000 points) were collected in an instrumented plot at one of the Castaño Viejo tailings dams (different from the study case). The measurements correspond to a silt layer in the beach zone, located 7 cm below the surface. The instrumentation consisted of a Decagon MPS-2 suction sensor and a Decagon 5TE volumetric moisture sensor. The dry unit weight of the layer was also measured, converting volumetric moisture readings to degree of saturation for inclusion in Figure 8. The retention curve derived from field data shows higher suction values than laboratory samples for the same degree of saturation. This suggests that the field material is finer. One possible explanation for this discrepancy is again the strong heterogeneity of hydraulically deposited tailings.

Table 3. Parameters of eq. (1) fitted to the experimental data shown in Figure 8.

MATERIAL	*Discharge (Lab)*	*Beach (Lab)*	*Beach (in situ)*
α [kPa^{-1}]	*0.1667*	*0.0260*	*0.0043*
n	*1.695*	*1.345*	*1.559*
m	*0.410*	*0.257*	*0.359*
θ_r	*0.015*	*0.000*	*0.000*

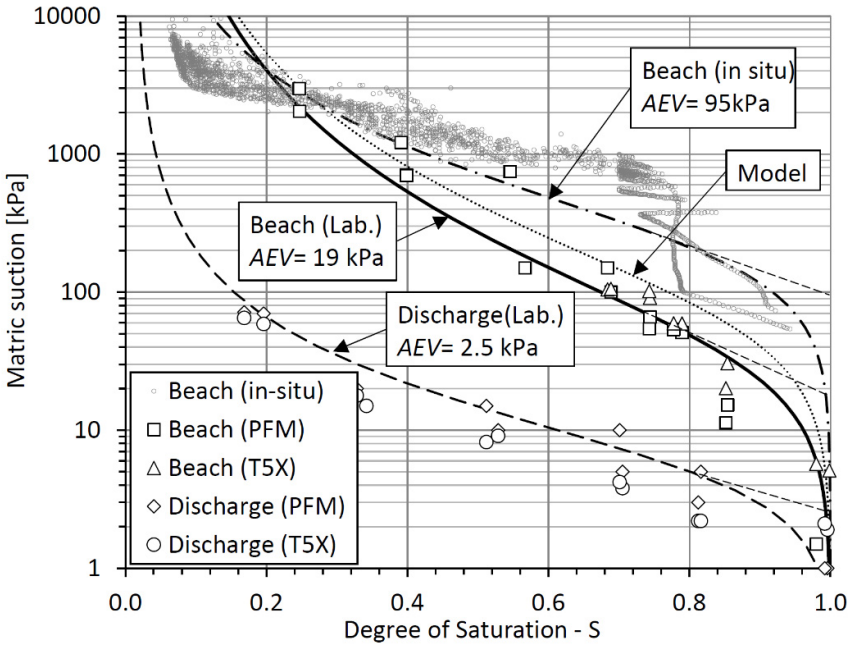

Figure 8. Retention curves of Castaño Viejo Tailings (data after [14, 15]). Laboratory specimens were prepared at a dry unit weight of 14.5 kN/m^3. van Genuchten (1980) [19] curves fitted to the experimental data with the parameters indicated in Table 3.

Shear Strength and Compressibility

Suction-controlled tests were not available for this study. However, estimating the additional strength arising from the unsaturated state is essential in this case. As follows from the experimental data and the restored deposit geometry, the main slope would not have been stable without the contribution of matric suction, favoured by the arid climate.

The shear strength was measured in direct shear tests with constant water content. The tests were conducted on remoulded specimens from samples gathered in the discharge zone and beach zone [9]. The mechanical properties of the tailings from the pond zone are not relevant to stability. For each specimen, the degree of saturation was computed from the initial water content and the void ratio computed at the end of the consolidation stage. The results of all tests performed are plotted in the shear stress vs. normal stress plane in Figure 9. Next to each test datapoint, the degree of saturation (at the initiation of the shear phase) is indicated. A moderate increase in the measured strength can be noticed with the decrease of the saturation degree. As expected, the effect is more intense in the beach silt than in the sand from the discharge zone.

For modelling purposes, the shear strength is described by means of the expression proposed by Vanapalli et al, 1996 [20].

$$\tau = c' + \left(\sigma - p_g\right)\tan\emptyset' + (\theta - \theta_0)/(\theta_s - \theta_0)\left(p_g - p_l\right)\tan\emptyset' \qquad (2)$$

where τ is the shear strength, c' is the cohesion for the saturated state, ∅' is the effective friction angle and σ is the applied normal stress. The third addend of eq (2) yields the apparent cohesion due to the capillary forces arising from the unsaturated state. The parameter θ_0 is a threshold volumetric water content value below which the apparent cohesion vanishes for dry conditions.

Eq. (2) shall be used with eq. (1) since the matric suction $(p_g - p_l)$ is determined by the retention curve for each value of θ. Figure 9.a displays, along with the experimental results, the Mohr-Coulomb (M-C) envelopes arising from eqs. (1) and (2) with the corresponding values of the parameters indicated in Tables 2 (last column for the beach material) and 4, respectively. Figure 9.b displays the variation of the apparent cohesion due to capillary forces with the degree of saturation. Apparent cohesion is computed as the y-intercept of an M-C envelope passing through each data point, assuming a fixed slope $(= \tan \emptyset')$ for each material. The data are compared to the plot of third addend of eq (2), computed with the corresponding set of parameters. The model predicts a vanishing apparent cohesion for very dry states, which is physically expected to occur, although it is not evidenced by the available set of data.

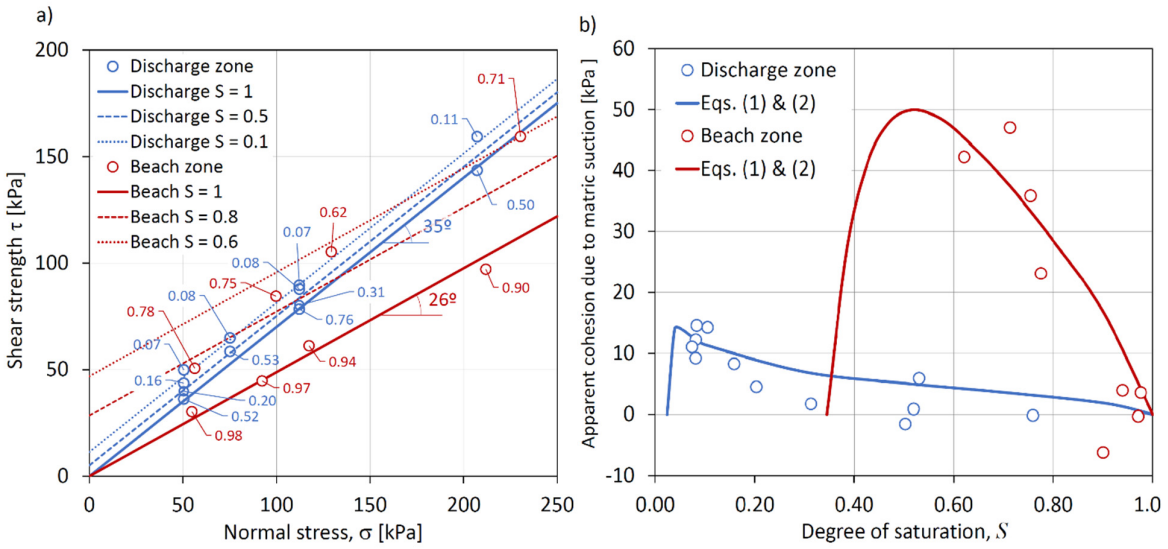

Figure 9. Shear strength determined in direct shear tests conducted under constant water content for the discharge zone sand and the beach silt (data after [14]). Laboratory specimens were prepared at a dry unit weight of 14.5 kN/m³. a) Experimental results obtained in direct shear tests with constant water content (initial degree of saturation indicated for each datapoint) and Mohr-Coulomb envelopes for given values of initial degree of saturation resulting from the application of eqs. (1) and (2) along with the parameters given in Tables 2 and 4. b) Measured apparent cohesion as a function of the initial degree of saturation compared to eq. (2) plot.

Finally, to calculate the saturated storage term in transient flow analyses, it is important to characterize the compressibility of the porous medium. The volumetric compressibility

modulus was measured in oedometric tests for the beach tailings. The value obtained in unloading/reloading paths, $m_v = 2.05E-05\ kPa^{-1}$ is adopted for all materials.

Table 4. Eq. (2) parameters for describing the variation of shear strength with the normal stress and matric suction.

MATERIAL	*Discharge zone*	*Beach zone*
ϕ' [º]	*35*	*26*
c'	*0.000*	*0.000*
θ_0	*0.012*	*0.159*

Modelling the failure process

Analysis section – Materials zonation

Analyses were conducted in two dimensions. The analysis section is shown in Figure 10 (its trace is indicated in Figure 2. b). The material zonation was adopted according to the restored deposit geometry and field observations. The materials considered are the three types of tailings already discussed in the previous sections, plus an alluvial fill in the valley bottom, the rockfill making up the starter dam and a zone of rockfill clogged with tailings in the upstream part of the starter dam. The tailings beach is assumed to have a uniform slope of 1% upstream. Otherwise, the slope of the valley bottom is 7.3%. The position and level of the decant pond was identified in the field by the marks in the tailings relicts. The section in Figure 10 includes the indication of the position of the decant pipe, the karstified tailings zone and the approximate geometry of the sliding surfaces interpreted from the field observations. The rock outcrops in the nearby of the deposit in both margins and in the stream bed at the position of the starter dam (igneous dike). Hence the alluvium is inferred to be shallow. A depth of 1 metre is assumed.

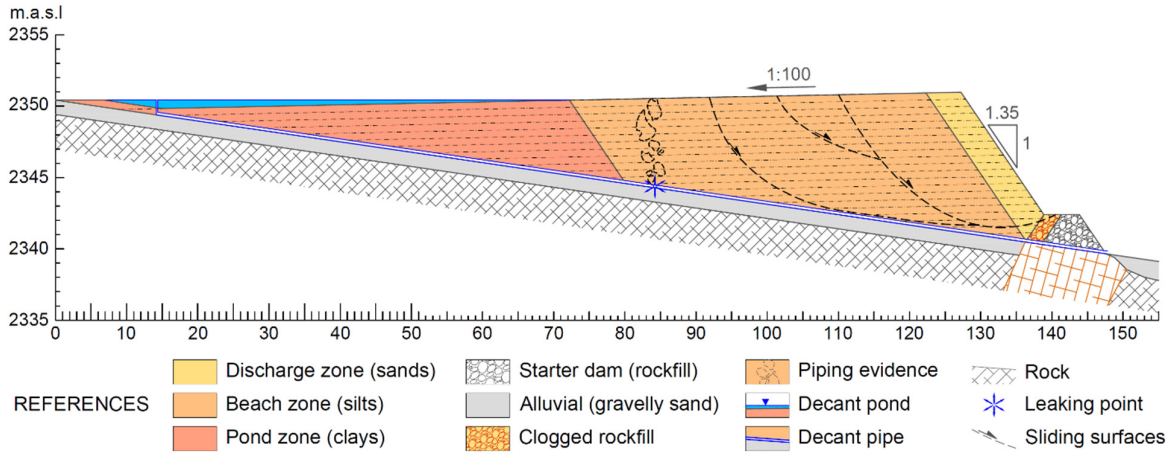

Figure 10. Analysis section for the base case. Vertical scale exaggerated by 2.

Material parameters

All material parameters adopted for the model are summarized in Table 5. The tailings parameters were selected according to the data shown in the previous sections. For the permeabilities, the field data were initially preferred to the determined in the laboratory. In an anisotropic medium the Boutwell Permeameter (ASTM D6391 Method B [16]) is expected to yield the geometrical mean of the horizontal, k_H, and the vertical, k_V, permeabilities [21]. According to the usual practice reported in the literature [22, 23], a ratio between the vertical and the horizonal permeability, k_V/k_H = 0.1 was adopted. Hence the vertical and horizontal permeabilities were determined by multiplying and dividing the field values by $\sqrt{3}$, respectively. Since the stratification has a slight dip directed upstream (1%), anisotropy axes are rotated 0.6º counterclockwise. For the beach tailings an intermediate retention curve was adopted, between the lab and the field curves presented in Figure 8, with AEV = 30 kPa.

Parameters for the alluvial material and the stater dam were adopted from the literature. The starter dam is basically composed by coarse grained rockfill, but a zone of its upstream part is clogged with tailings. Hence it was assumed in that zone the material is composed by a fine matrix of discharge tailings with clasts of solid rock, each occupying 50% of the volume. Therefore, the shape of the retention and relative permeability curves adopted are identical to the discharge tailings, but the porosity and the saturated permeability half the tailings values. For shear strength, identical parameters were adopted as those of the clean rockfill.

Table 5. Parameters for failure modelling

Constitutive Law	*Parameter*	*TAILINGS*			*Alluvial Fill*	*STARTER DAM*	
		Disch.	*Beach*	*Pond*		*Clogged rockfill*	*Rock-fill*
Physical properties	γ_d[kN/m³]	14.80	15.00	13.70	16.00	21.30	14.00
	θ_s	0.48	0.46	0.44	0.40	0.24	0.50
Hydraulic Cond. Darcy	k_{Hsat} [m/s]	3.1E-6	5.4E-7	1.9E-7	1.0E-5	1.5E-6	1.E-3
	k_V/k_H	0.1	0.1	0.1	0.1	1.0	1.0
	Dip [º]	-0.6	-0.6	-0.6	4	---	---
Retention Curve & Relative permeability van Genuchten 1980 [19]	α [kPa^{-1}]	0.1667	0.0143	0.01	---	0.1667	1
	n	1.695	1.370	1.3	---	1.695	4
	θ_r	0.007	0	0	---	0.003	0
	m_V [kPa^{-1}]	2E-05	2E-05	2E-05	2E-05	2E-05	---
Shear strength Mohr-Coulomb + Vanapalli et al. 1996 [20]	ϕ' [º]	35	26	26	35	40	40
	c' [kPa]	0.00	0.00	0.00	0.00	0.00	0.00
	θ_0	0.012	0.159	---	---	---	---

Modelling stages

Each model comprises three stages: 1) a steady-state finite element model for analysing seepage in steady state regime under normal operation, to obtain the failure-precedent condition.2) A transient seepage finite element model, with the decant pipe injecting water under pressure at the point where the piping phenomena was observed, being the hydraulic head at the injection point determined by the pond level. 3) A limit equilibrium analysis at the steady-state- stage and at each time-step of the transient analysis with the goal of detecting the onset of instability. Modelling was carried out with GeoStudio software.

Discussion of model results

Explaining failure turned to be not straightforward. In fact, no failure was predicted with the Base Case model which uses the geometry of Figure 10 and the parameters of Table 5. The minimum factor of safety after running the steady-sate stage was 1.6. After running the transient stage during a six-month period injecting water from the leaking pipe, a minimum safety factor of 1.3 was attained with the model approaching a new steady state flow condition. Hence a series of additional factors were tested to understand the failure mechanism. Those factors are discussed in the following sections and incorporated into a new model, termed the Failure Case. The goal was to weight out their relative importance in the failure process.

Drainage issues at downstream toe

Following the field observations a zone of rockfill clogged with tailings was already included in the Base Case model. The results of the analysis suggest that a more severe restriction to drainage is required at the dam toe to water pressure buildup beneath the slope and thus triggering the instability. Possible drainage issues can arise from the way the first pours of tailings are carried out. Due to the small space available, the firsts lifts are poured over a short beach or no beach at all. Hence no segregation occurs during those first stages and the zone next to starter dam becomes filled with all-in-one-tailings slurry. Thus, a sort of plug of low permeability material is built right in the place where the highest permeability tailings are supposed to provide good drainage. This violates the basic assumptions of healthy working upstream raised dams [23]. Notably, the failure cases of Correio de Feijao (Brumadinho) [11, 12] and Fundão dams [24], both upstream raised, involved severe and chronic drainage issues in the vicinity of their downstream toe. As depicted in Figure 12.d, a wedge of low permeability material was introduced in the model next to the starter dam.

Tailings heterogeneity, stratification and permeability anisotropy

Tailings deposits built by hydraulic deposition comprise two broad types of materials: 1) beach tailings, with particle sizes ranging from sands to silts, sorted by particle sizes while spreading over the beach and 2) the slimes, which is the fines fraction of the tailings particles, containing silt and clay particles. Beach tailings deposition is subaerial while slimes deposition is subaqueous. The formation mechanisms of such a layered structure are pretty like those of natural deltaic deposits [25]. The exploration of ancient tailings deposits [8-10,14] and failure cases like Mount Polley [26], Fundão [27] and Correio de Feijao [12] show that their internal structure can be highly heterogeneous. It is common to observe stratified tailings with juxtaposed layers of highly contrasting grain size, both in the beach and in the decant pond zone. Strata thicknesses

vary from decimetres to millimetres and normally display a gentle dip in the upstream direction, which is more pronounced in the decant pond zone [28].

The concept of upstream raised tailings dams [23, 29] implies that the deposited tailings ideally have increasing grain sizes in downstream direction which grant a rising permeability towards the dam. This feature should grant a low position of the phreatic surface, away from the dam outer slope. Permeability anisotropy of tailings must be considered. Vick (1990) reports that the common range of the ratio k_V/k_H is 0.5 to 0.1, but it could be lower (0.01 or less) in the case beach tailings and slimes become interlayered [23]. Interlayering, i.e. the inclusion of slimes layers interspersed between tailings layers, is caused by the fluctuations in the level of the decant pond. For instance, there is evidence that the tailings beach of most of the failure cases mentioned in the previous paragraph resulted completely flooded, possibly many times during their lifetime, and displayed interlayering [11, 12, 26, 27]. Beach flooding the inhibition of the particle size sorting mechanism and the deposition of slimes all over the area covered by water.

The Failure Case model considers higher-than-normal anisotropy ratios for the tailings permeability. It is assumed that lab tests on reconstituted specimens (wet tamped) yield values roughly close to the vertical permeability, k_V. This is a reasonable hypothesis since the permeability is controlled by the finer fraction, i.e., the tailings arising from the fine-grained strata. Moreover, as in the Base Case, the field measurements (Boutwell permeameter) are considered the geometric mean of k_H and k_V [21]. Thus, the corresponding k_H values can be inferred from these two assumptions. All permeability values are depicted in Figure 11 as a function of the distance between the dam crest and the sampling point. The resulting ratio k_V/k_H is in the order of 10^{-2} for the sand of the discharge zone and of 10^{-3} for the beach and the pond zones. It is interesting to note that the permeability data collected for the analysis of the Correio de Feijao accident [11] support such a three-orders-of-magnitude variability range in any vertical within the beach zone.

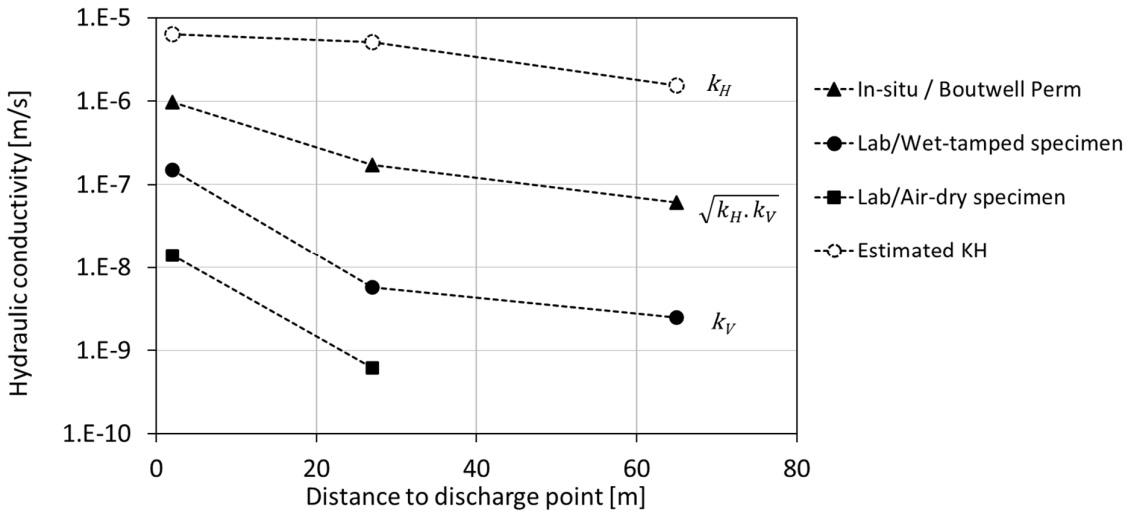

Figure 11. Hydraulic conductivity measurements as a function of the distance from the discharge point (dam crest) were the sample or measurement was taken (values indicated in Table 2). Horizontal permeability estimated according to the hypotheses made in the Failure Case Model.

Surficial drying, shrinkage, salt precipitation and capillary rise

Tailings air-drying occurs at the surfaces of the deposit, both at the outer slope and at the top of the tailings beach. Tailings particles range between fine sand and a silt, and their GSDs are rather uniform. Consequently, as the surficial layer dries off, its hydraulic conductivity falls dramatically. In an arid climate, like the case studied, the potential evaporation easily exceeds liquid flux reaching the surface by capillary rise. The resulting water imbalance in a shallow depth layer leads to the formation of a dry crust. At some point the liquid phase loses its continuity, the flux of liquid water drops to zero, and the only remaining mechanism of water transport is vapour diffusion. Thus, the dry crust becomes nearly watertight, while the inner body of tailings attains wetter states due to capillary rise under nearly hydrostatic conditions. Field surveys show that many ancient tailings deposits comprise a inner body of soft tailings which remain in a more o less permanent wet state, enclosed by an outer dry and hard shell [7, 10, 15]. Observed thicknesses of the dry shell range 1 to 2 m. The precipitation of salts eventually adds some amount of cementation to the dry shell, eventually enhancing its strength. At the same time the clogging of pores by precipitated salts decreases even more its permeability, as suggested by the experiments (Figure 11)

To test the effect of surficial drying while keeping the analysis simple, two matric suction values conveniently chosen were imposed on all boundaries exposed to atmospheric action: 1 MPa and 10 MPa, in the Base Case and the Failure Case, respectively. Those matric suctions were applied to the finite element seepage model imposing negative liquid pressures as forced (Dirichlet) boundary conditions. Such boundary conditions produced the expected effects, i.e., the Base Case model mimicked a mild evaporative flux fed by capillary rise from the phreatic surface, while under the harsh evaporation condition in the Failure Case model, a dry shell evolved, cutting off the evaporation despite the higher suction applied (Figure 12.a and b, respectively). Consistently, the evaporative flux obtained in the steady state stage of the analysis was 0.07 mm/day and 0.01 mm/day in the former and later case, respectively. Both values are well below the daily mean potential evaporation measured at the site, which is 3.4 mm. In addition, a distinct material shell was incorporated in the transient analysis stage, to simulate the reduced permeability due to shrinkage and salt precipitation, according to the experimental results presented above. The permeabilities adopted for such shell materials are the obtained in the lab tests (Table 2).

Case analysis and closing discussion

The incorporation of the three factors discussed above into the model allowed reaching a sliding failure within 6 days after initiating water injection from the leaking pipe (Figure 12.d). Moreover, six additional cases were run in which the factors were removed one by one (Cases A, B, and C) and added one by one (Cases D, E, and F), respectively. The hypotheses and results of all the analyses performed are summarised in Table 6. For instance, removing factor 1 (Case A) or factor 3 (Case B) increases the time-to-failure to 10 or 15 days, respectively. Removing only factor 2 (Case C) from the model yields no failure. Otherwise, leaving only factor 1 (Case D) or factor 2 (Case E) yields no failure, while the single influence of factor 2 leads to failure, but delayed 40 days after initiating water injection. Hence it can be concluded that including the strong anisotropy of tailings is necessary and sufficient for failure, the other two factors acting as accelerators of the failure process. From the safety perspective, the shorter the time-to-failure, the more dangerous the incident is.

The physical effects of the three factors on the model response can also be qualitatively analysed (refer to Figure 12).

Including the low permeability plug next to the starter dam (Factor 1) delays the drainage in a zone right beneath the main slope, enhancing the rise of pore pressures, which will eventually trigger the slide.

Stratification, included in the model as a strong anisotropy of permeability (Factor 2), has a double effect. Regarding the failure-precedent condition, the permeability anisotropy causes the beach tailings to be fed by capillary water coming directly from the pond zone(compare Figures 12.a and 12.c). This means that the beach tailings body is permanently kept close to saturation, no matter if the phreatic surface has a low position. The analysis of the Correio de Feijao accident [3] arrived at similar results. Having a beach zone almost saturated as a failure-precedent condition means that injection (or seepage/infiltration) of a relatively small amount of water is enough to bring the liquid pressures to positive values and hence facilitate the development of the unstable conditions. A second effect of permeability anisotropy in the particular failure mechanism analysed here is that the injection pressure from the leaking pipe is more readily transmitted to the downstream zone close to the main slope (Figure 12.d).

Finally, the harsh drying boundary condition and the development of a dry and low-permeability shell (Factor 2) also have a double effect. During the steady-state analysis, the low permeability shell also contributes to the formation of a close-to-saturated body of beach tailings, as explained in the previous section (Figure 12.c). During the transient analysis, the dry shell delays the seepage at the toe of the main slope, hence accelerating the development of the unstable conditions and excluding the possibility of the operator to have a hint of the incident evolving (Figure 12.d).

Table 6. Analysis cases. Summary of hypotheses and results.

CASE	*FACTORS*			*Analysis Result / Time-to-failure*
	1 - First pour low permeability plug	*2 - Stratification - Strong anisotropy of permeability*	*3 - Harsh drying BC + Shrinkage & Precipitation Crust*	
BASE	X	X	X	*No failure*
FAILURE	✓	✓	✓	*6 days*
A	X	✓	✓	*10 days*
B	✓	✓	X	*15 days*
C	✓	X	✓	*No failure*
Necessary for failure?	*NO*	*YES*	*NO*	
D	✓	X	X	*No failure*
E	X	X	✓	*No Failure*
F	X	✓	X	*40 days*
Sufficient for failure?	*NO*	*YES*	*NO*	

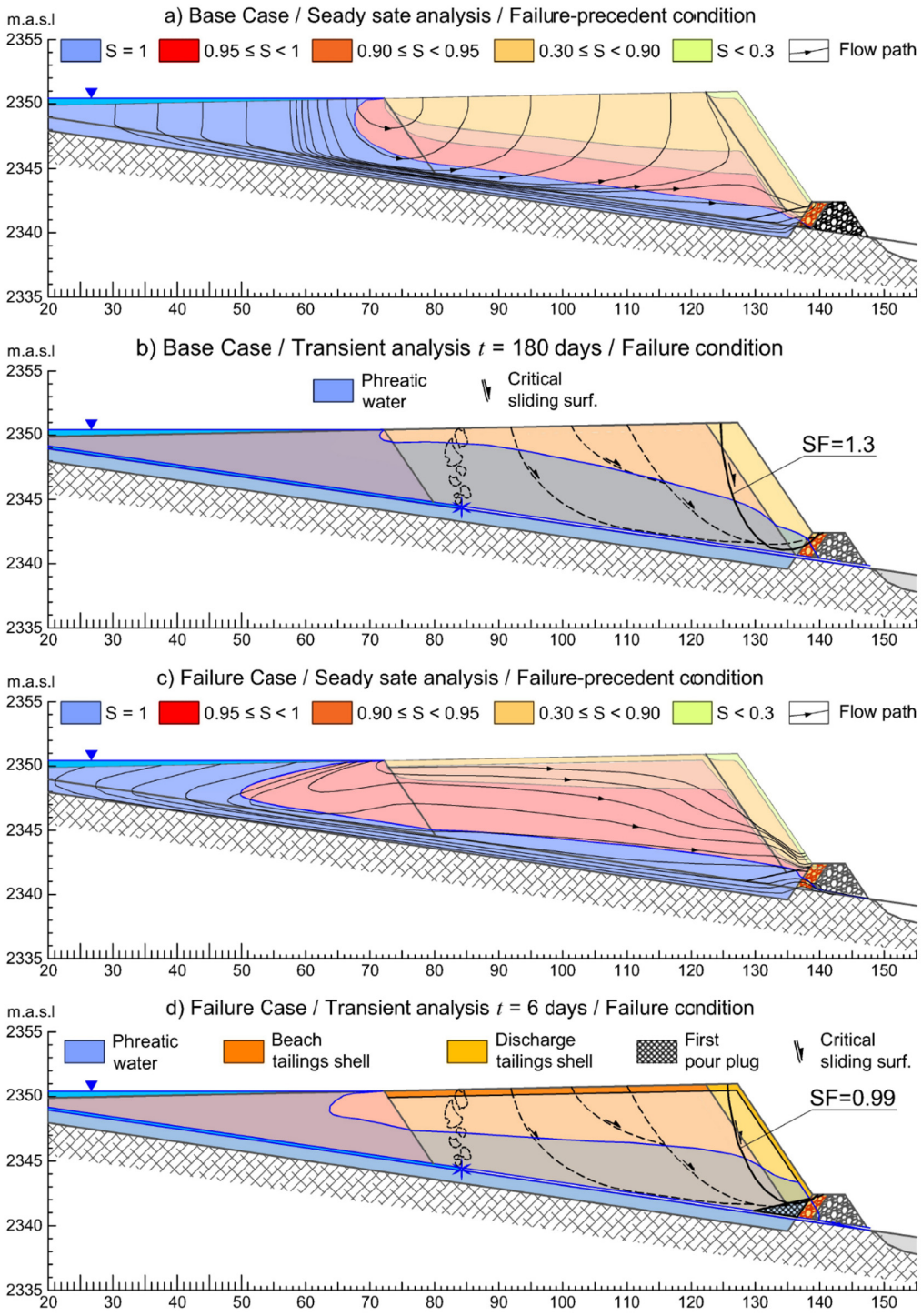

Figure 12. Model results. a) Base Case: steady-state seepage analysis. b) Base Case: Transient seepage and limit equilibrium analyses. c) Failure Case: steady-state seepage analysis. d) Failure Case: Transient seepage and limit equilibrium analyses (refer to Figure 11 for missing references). Vertical scale exaggerated by 2.

Conclusions

It seems likely that the cause for the Upper Castaño Viejo failure was the malfunctioning of the decant system. This type of failure has occurred with some frequency throughout the world. The model shows how dangerous this type of installation was, today fortunately almost in disuse.

However, explaining the failure was not straightforward. Additional hypotheses had to be made. Among the studied factors, permeability anisotropy seems to play a primary role in the development of the unstable conditions for the case studied here. This feature is usually considered a second-order factor in forecasting the performance of tailings dams, while this study suggests that it may have a primary role. The analysis presented here considers a limited number of factors among those which possibly could determine the performance of the dam. Other factors, like the alluvial permeability or the shape of the relative permeability curve of all materials, could also have a significant role in the failure process.

The analysis presented also shows that unsaturated phenomena play a role in the failure mechanism, particularly in determining the failure-precedent condition which is determinant of the possibility of effectively developing a failure and the time required for the failure to occur. Because of the tailings stratification, which makes them a very heterogeneous material, there is a nearly unavoidable uncertainty associated with the hydraulic characterization of tailings, particularly in the unsaturated range.

From a more general perspective, the case practically shows the complexity of upstream-raised tailings, with multiple phenomena and factors that determine their performance. This makes guessing their failure mechanism a tortuous task and hence very challenging. It seems quite unlikely for an analyst to forecast the failure process described in this paper, for instance. In spite of modern dams being quite different from the old ones, they are no less complex. The basic way to analyse their safety, like in any other engineering work, is basically to assume a series of failure mechanisms and then verify the safety margin with respect to each failure scenario. If, as this work suggests, guessing the failure mechanisms is so difficult, chances exist that failures occur due to mechanisms that were never imagined nor verified. This seems to be just the case in some recent tailings dam failures with worldwide repercussions.

Acknowledgements

The analysis in this paper was generated using Seequent software GeoStudio. Seequent is the Bentley Systems subsurface company. Copyright ©2024 Bentley Systems, Incorporated.

References

[1] F.J. Fernández-Naranjo, V. Rodríguez-Gómez, R. Rodríguez, M.E. Alberruche del Campo, J.C. Arranz-González, L. Vadillo. Liquefaction susceptibility assessment and study of "La Luciana" tailings dam fault (Spain, 1960) based on historical documents. *Dyna* 82(189):189–198, 2015.

[2] J.L. Berzal. Presas de residuos mineros. *Revista de Obras Públicas* 123 (3131), pp. 301-333, 1976.

[3] G. Villavicencio, R. Espinace, J. Palma, A. Fourie, P. Valenzuela. Failures of sand tailings dams in a highly seismic country. *Can Geotech J,* 51(4):449–64, 2013.

[4] L. Valenzuela, L. (2015). Tailings Dams and Hydraulic Fills – The 2015 Casagrande Lecture. Geotechnical Synergy in Buenos Aires, pp. 5-49, 2015.

[5] D.J. Williams. Lessons from Tailings Dam Failures—Where to Go from Here? Minerals. 2021, 11, 853. https://doi.org/10.3390/min11080853

[6] Wang, C., Harbottle, D., Liu, Q. and Xu, Z. Current state of fine mineral tailings treatment: A critical review on theory and practice. *Minerals Engineering* 58,113–131, 2014

[7] Rodríguez R, García C, Zarroca M, Oldecop, L. Características geológicas y geotécnicas de los lodos de flotación de la Sierra Minera de Cartagena-La Unión (SE España). Boletín Geológico y Minero 122(2): 127–144, 2011

[8] Rodríguez, R., Muñoz, A., Caparrós, V., García, C., Brime, A., Arranz, J., Rodríguez, V., Fernández, F., Alcolea, A. How to Prevent Flow Failures in Tailings Dams. Mine Water Environ 40, 83–112, 2021

[9] Garino L., Rodari G., Oldecop L. Characterization of mine waste materials after 50 years of climate interaction. Second Pan-American Conference on Unsaturated Soils, Dallas, United States, 2017.

[10] R. Rodríguez-Pacheco, R. A.V. Caparrós, A. Alcolea, P. Martínez-Pagán, M.A. Martínez-Segura, C. García-García, Á. Faz, I. Corral, C. Roque, M. Zarroca. Static Liquefaction Causes the Flow Failure of a Tailings Dam: A Case Study of El Descargador Cartagena–La Unión Mining Region, SE Spain (October 1963). Minerals 2022, 12, 1488.

[11] M Arroyo and A Gens. "Computational Analyses of Dam I Failure at the Corrego de Feijao Mine in Brumadinho. CIMNE. Final Report for VALE S.A, 2022.

[12] PK Robertson, L de Melo, DJ Williams & GW Wilson. Report of the expert panel on the technical causes of the failure of Feijão Dam I. http://www.b1technicalinvestigation.com/ [accessed Jan 03 2025].

[13] AJ Whittle, HM El-Naggar; SA Y. Akl, AM Galaa. Stability Analysis of Upstream Tailings Dam Using Numerical Limit Analyses. J. Geotech. Geoenviron. Eng., 2022, 148(6). https://doi.org/10.3390/min12121488

[14] L. Garino. Estudio del comportamiento mecánico e hidráulico de depósitos de residuos mineros ubicados en zonas áridas. Doctoral Thesis. Universidad Nacional de San Juan, 2018.

[15] L. Garino Libardi and L. Oldecop. Evolución de la humedad en presas de relaves mineros ubicadas en climas áridos. Caso de estudio: mina Castaño Viejo, San Juan, República Argentina, *Boletín Geológico y Minero de España*, 132 (4), 487-507, 2021. DOI: 10.21701/bolgeomin.132.7.004

[16] ASTM. D6391-11 Standard Test Method for Field Measurement of Hydraulic Conductivity Using Borehole Infiltration. ASTM International, West Conshohocken, PA, 2011.

[17] ASTM. D5084-16 Standard Test Methods for Measurement of Hydraulic Conductivity of Saturated Porous Materials Using a Flexible Wall Permeameter. ASTM International, West Conshohocken, PA, 2016.

[18] ASTM. D5298-92 Standard test method for measurement of soil potential (suction) using filter paper. ASTM International, West Conshohocken, PA, 1992.

[19] M. Th. van Genuchten. A closed-form equation for predicting the hydraulic conductivity of unsaturated soils. *Soil Sci. Soc. Am. J.* 44:892-898, 1980

[20] S. K. Vanapalli, D.G. Fredlund, D.E. Pufahl and A.W. Clifton. Model for the prediction of shear strength with respect to soil suction. Can. Geotech. J. 33, No. 3, 379–392, 1996.

[21] MJ Hvorslev. Time Lag and Soil Permeability in Groundwater Observations. Waterways Experiment Station, Corps of Engineers, US Army Bulletin 36, Vicksburg MS, 1951.

[22] JP Welch. Water fow through tailings dams. PhD thesis, Durham University, 1993. http://etheses.dur.ac.uk/5523/

[23] SG Vick. Planning, Design and Analysis of Tailings Dams, Wiley Interscience, John Wiley & Sons, New York, 1990.

[24] Morgenstern, N. R.; Vick, S. G.; Viotti, C. B.; Watts, B. D. Fundão Tailings Dam Review Panel, Report on the Immediate Causes of the Failure of the Fundão Dam. 2016. https://www.resolutionmineeis.us/documents/fundao-2016 [accessed January 14, 2025]

[25] GE Blight & GM Bentel. The behaviour of mine tailings during hydraulic deposition. J. S. Afr. Inst. Min. Metal/., vol. 83, no. 4. Apr. 1983. pp. 73-86.

[26] Independent Expert Engineering Investigation and Review Panel. 2015. Report on Mount Polley Tailings Storage Facility Breach. Government of British Columbia, 30 January 2015. https://www.mountpolleyreviewpanel.ca/ [accessed January 14, 2025]

[27] Morgenstern, N. R.; Vick, S. G.; Viotti, C. B.; Watts, B. D. Fundão Tailings Dam Review Panel, Report on the Immediate Causes of the Failure of the Fundão Dam. 2016. https://www.resolutionmineeis.us/documents/fundao-2016 [accessed January 14, 2025]

[28] B. H. Conlin. `Tailings beach slopes', in Geotechnical Aspects of Tailings Disposal and Acid Mine Drainage, The Vancouver Geotechnical Society, 1989.

[29] TE Martin & E.C. McRoberts "Some considerations in the stability analysis of upstream tailings dams. Tailings and Mine Waste ’99, Fort Collins, Colorado, pp. 287-302, 1999.